

# Magnesium Triimidosulfonates from Grignard Reagents

Thomas Schulz<sup>[a]</sup> and Dietmar Stalke<sup>\*[a]</sup>

**Keywords:** Sulfur / Imides / Magnesium / Grignard reaction / Structure elucidation

The triimidosulfonate complexes  $[(\text{thf})\text{MgX}(\text{NtBu})_3\text{SR}]_2$  (**1**: R = methyl, X = Br; **2**: R = *n*-butyl, X = Cl; **3**: R = phenyl, X = Cl; **4**: R = benzyl, X = Cl) can be obtained very pure and in good yield upon treatment of the sulfur triimide  $\text{S}(\text{NtBu})_3$  with the appropriate Grignard reagent  $\text{RMgX}$ . Changing the solvent from thf to toluene results in elimination of  $\text{MgBr}_2$  from **1** and generates the new complex  $[\text{Mg}\{(\text{NtBu})_3\text{SMe}\}_2]$  (**5**). Complexes **1–5** should be good precursors for a variety of heterobimetallic complexes since transmetallation reac-

tions are well established for this compound class and the third imido group is in an ideal position to coordinate a second metal. The triimidosulfonate ligands accommodate the requirements of the added organic group by either changing the twist between both ligands in the dimer or even changing the structural motif, as exemplified by **3**. NMR investigations in solution confirm this conformational freedom and the adaptability of these ligands to a metal as electronically "hard" as magnesium.

## Introduction

Sulfur is one of the most versatile elements in main group chemistry, with sulfur oxides showing a particularly interesting chemistry and a variety of coordination patterns.<sup>[1]</sup> Isoelectronic replacement of the oxygen atoms in these compounds with RN groups leads to new molecular architectures. The first sulfur diimide  $\text{S}(\text{NtBu})_2$ , the RN-substituted analogue of sulfur dioxide, was reported by Goering and Weis in 1956,<sup>[2]</sup> and 14 years later Glemser and Wegener<sup>[3]</sup> succeeded in synthesizing the first analogue to sulfur trioxide, namely the sulfur triimide  $\text{S}(\text{NSiMe}_3)_3$ .<sup>[4]</sup> Since then much effort has been dedicated to investigating this new compound class and their coordination properties, although progress in this field was often hampered by the limited synthetic access to imidosulfur molecules. Until 1996, when our group reported a new synthetic approach,<sup>[5,6]</sup> only two reactions were known starting from  $\text{NSF}_3$ <sup>[7]</sup> or  $\text{OSF}_4$ <sup>[8]</sup> which are quite hazardous and give only poor yields. Since then the group of Chivers et al.,<sup>[9]</sup> as well as our group, have investigated the bonding situation<sup>[10–12]</sup> and the coordination pattern of *tert*-butylsulfur triimide<sup>[13]</sup> and the associated organosulfur triimidosulfonates.<sup>[14–17]</sup> One advantage of sulfur triimides over sulfur diimides is their additional coordination site, which can be employed in the synthesis of heterobimetallic complexes.<sup>[16]</sup> Furthermore, sulfur triimides can be connected via an organic spacer, with a methylene group<sup>[11]</sup> and heteroaromatic bridges<sup>[17]</sup> having already been employed for this purpose. It should even be possible to incorporate three or four dif-

ferent metals in one complex by connecting two molecules.

These compounds also have their drawbacks however. For example, the nucleophilic attack required to generate the desired organotriimidosulfonate is only possible with small or planar nucleophiles. An explanation for this based on steric factors steric would not be possible if direct orthogonal attack above or below the  $\text{SN}_3$  plane was favoured as there is sufficient room to attack the sulfur atom directly (see Figure 1). The reactive surface, however, shows areas of strong charge depletion in the  $\text{SN}_3$  plane at the bisections of the N–S–N angles at the sulfur atom and no hole either above or below the sulfur atom.<sup>[12]</sup> The carbanionic nucleophile therefore has to approach the sulfur atom along the NSN bisection in the  $\text{SN}_3$  plane or at an angle of less than about 45°, which is only feasible for small or planar carbanions. Bulky anions cannot reach the holes due to the steric hindrance of the *NtBu* groups in the equatorial region of the trigonal planar molecule.

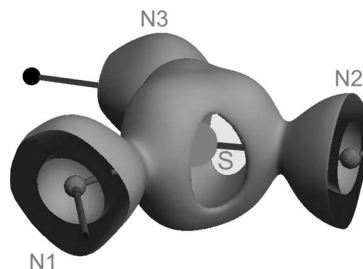


Figure 1. Reactive surface of  $\text{S}(\text{NtBu})_3$ .

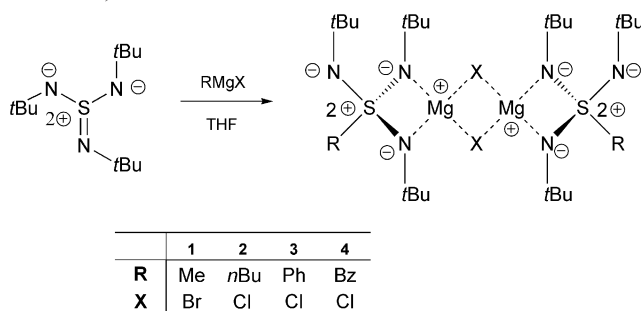
Our approach to tackle this problem was to employ Grignard reagents. Since organolithium reagents, the most frequently used nucleophiles, are rather hard according to Pearson,<sup>[18]</sup> we anticipated that the soft–soft interaction between an organomagnesium reagent and the sulfur atom

[a] Institut für Anorganische Chemie, Georg-August Universität Göttingen, Tammannstr. 4, 37077 Göttingen, Germany  
Fax: +49-551/393459  
E-mail: dstalke@chemie.uni-goettingen.de

would facilitate a reaction even with sterically more demanding substituents. In addition to their softer character, Grignard reagents are less reactive than their organolithium counterparts, which would also result in fewer side reactions and higher yields of the desired triimidosulfonates. A similar approach has already proved to be valid in the addition reaction of Grignard reagents to sulfur diimides.<sup>[19]</sup> This hypothesis proved to be resilient and it was possible to introduce a variety of organic groups into the triimidosulfonates. Thus, it is now possible to employ non-planar and sterically more demanding groups to connect two sulfur triimide residues and to vary the steric demand of the triimidosulfonate ligands by utilizing Grignard reagents. Some examples are presented in this paper.

## Results and Discussion

The triimidosulfonates  $[(\text{thf})\text{MgX}(\text{N}t\text{Bu})_3\text{SR}]_2$  (**1**: R = methyl, X = Br; **2**: R = *n*-butyl, X = Cl; **3**: R = phenyl, X = Cl; **4**: R = benzyl, X = Cl) synthesised herein are valuable precursors for heterobimetallic complexes, which are known to be good catalysts for many different reactions.<sup>[20]</sup> Thus, metal–metal exchange with halides or bis(trimethylsilyl)amides allows the magnesium atom to be substituted by a variety of metals,<sup>[15,21]</sup> and it is possible to introduce a second metal atom into the complex,<sup>[16]</sup> to form the desired heterobimetallic complex, by coordination to the third imido group of the triimidosulfonate. Compounds **1–4** can readily be synthesized simply by adding the Grignard reagent to the *tert*-butyl-substituted sulfur triimide (see Scheme 1).



Scheme 1. Preparation of the magnesium triimidosulfonates **1–4**.

This reaction is straightforward and the products crystallize very well, which means that the desired magnesium triimidosulfonates can be obtained in good yields and high purity after one or two days' storage in a freezer. Removal of the thf by evaporation and addition of toluene to the remaining solid generates new complexes of the general formula  $[\text{Mg}\{(\text{N}t\text{Bu})_3\text{SR}\}_2]$ . The resulting  $\text{MgX}_2$  salt can be removed by filtration and this approach gave  $[\text{Mg}\{(\text{N}t\text{Bu})_3\text{SMe}\}_2]$  (**5**) as colourless plates from a solution of **1** in toluene.

### Crystal Structures of the Magnesium Triimidosulfonates **1–5**

Selected bond length and angles for **1–5** are listed in Tables 1 and 2, respectively, and crystallographic data can

be found in the Experimental Section (Table 3). In contrast to most of their diimidosulfinate analogues, complexes **1–4** crystallize only as dimers, albeit with small differences in their general structural motif. Thus, two ligands are coupled by a central four-membered  $\text{Mg}_2\text{X}_2$  ring, with the magnesium atoms exhibiting a distorted square-pyramidal coordination polyhedron made up from two nitrogen atoms of the triimidosulfinate monoanion, one oxygen atom of a thf molecule and the two halogen atoms in all structures. All sulfur atoms show a distorted tetrahedral environment with very similar angles in all compounds. The uncoordinated *N**t*Bu group is pointing away from the metal atom and seems to be in an ideal position to coordinate a second metal (see Figure 2).

Table 1. Selected bond lengths [Å] for compounds **1–4**.

Compound	1	2	3	4
S–N1/N3	1.5808(21)	1.5949(23)	1.5880(21)/ 1.6017(19)	1.5948(20)/ 1.5969(20)
S–N2/N4	1.5976(17)	1.6075(22)	1.5976(19)/ 1.5880(21)	1.5936(20)/ 1.5967(20)
S–N5/N6	1.5228(21)	1.5282(22)	1.5281(22)/ 1.5224(20)	1.5271(20)/ 1.5257(20)
C–S1/S2	1.7880(22)	1.8107(26)	1.7972(32)/ 1.7972(25)	1.8310(24)/ 1.8331(24)
Mg–N1/N3	2.0650(19)	2.0692(23)	2.0666(21)/ 2.0777(21)	2.0941(21)/ 2.0903(21)
Mg–N2/N4	2.0677(20)	2.0712(21)	2.0774(20)/ 2.0821(20)	2.0703(22)/ 2.0898(21)
X1–Mg1/Mg2	2.6683(9)	2.4544(11)	2.4524(10)/ 2.5165(10)	2.4367(13)/ 2.4859(11)
X2–Mg1/Mg2	2.5947(9)	2.4874(11)	2.4249(10)/ 2.5178(9)	2.5134(11)/ 2.4621(11)
Mg–O	2.0325(18)	2.0712(21)	2.0537(18)/ 2.0452(18)	2.0606(19)/ 2.0645(20)

Table 2. Selected torsion angles and angles between planes for **1–4**.

Compound	1	2	3	4
$\text{Mg}_2\text{X}_2$ –N1S1N2	50.70	35.3	66.50	42.50
$\text{Mg}_2\text{X}_2$ –N3S2N4	50.70	35.3	37.00	35.20
N1S1N2–N3S2N4	0.00	0.00	101.10	24.00
S1Mg1Mg2S2–N1S1N2	73.50	82.10	46.40	72.40
S1Mg1Mg2S2–N3S2N4	73.50	82.10	79.00	83.70
N1–Mg1–Mg2–N3	75.03	74.20	33.52	58.15
N2–Mg1–Mg2–N4	75.03	74.20	44.04	97.36
X–Mg–Mg–N1	62.84	49.02	9.95	21.77
X–Mg–Mg–N2	12.19	25.18	82.14	55.04
X–Mg–Mg–N3	62.84	49.12	43.47	42.33
X–Mg–Mg–N4	12.19	25.45	38.10	36.38

As mentioned above, analogous diimidosulfonates mainly crystallize as monomers with a second donor molecule substituting the second halogen atom in the square-pyramidal coordination geometry—only when the organic groups are large or inflexible is a dimeric form favoured. Since the triimidosulfonates possess a third *N**t*Bu group, the steric demand of the ligand is too large for a second donor molecule

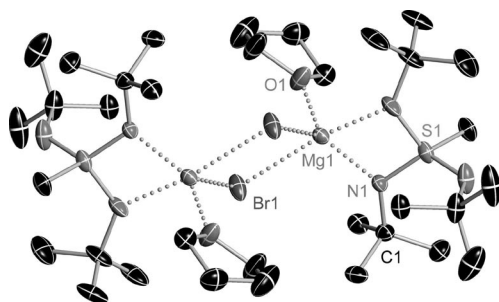


Figure 2. Crystal structure of  $[(\text{thf})\text{MgBr}(\text{N}t\text{Bu})_3\text{SMe}]_2$  (**1**). Anisotropic displacement parameters are depicted at the 50% probability level and all hydrogen atoms have been omitted for clarity.

and only dimeric structures are formed. Changing the organic group therefore makes virtually no difference to the general structural motif, and changing the halogen atom in the central ring has no major impact on the overall structure either (see Figure 3).

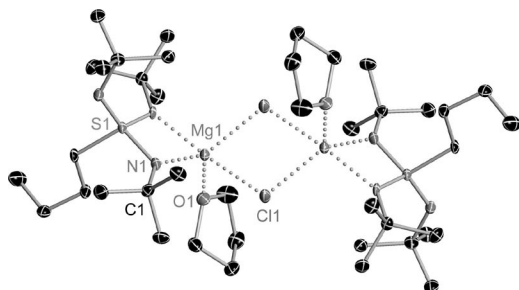


Figure 3. Crystal structure of  $[(\text{thf})\text{MgCl}(\text{N}t\text{Bu})_3\text{SnBu}]_2$  (**2**). Anisotropic displacement parameters are depicted at the 50% probability level and all hydrogen atoms have been omitted for clarity.

Both the general structural motifs (see Figure 4) and most of the bond lengths and angles are identical, within their estimated standard deviations, for complexes **1**, **2** and **4**. The minor differences observed include, for example, an elongation of the S–C bond length in **4** due to the electron-withdrawing effect of the phenyl substituent. The differences in the Mg–X and Mg–O bond lengths in **1** most probably result from the switch from bromine to chlorine.

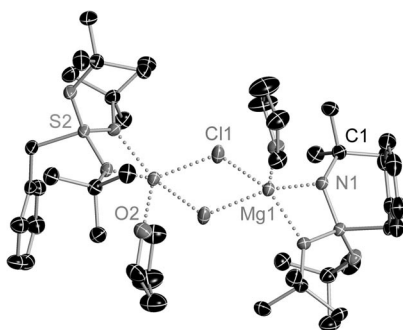


Figure 4. Crystal structure of  $[(\text{thf})\text{MgCl}(\text{N}t\text{Bu})_3\text{SBz}]_2$  (**4**). Anisotropic displacement parameters are depicted at the 50% probability level and all hydrogen atoms have been omitted for clarity.

A comparison of the monomeric structural motif of the diimidosulfonates and the dimeric motif of the triimidosulfonates (see Figure 5) shows that changing the added organic substituent has a more substantial impact on the solid-state structure of the latter.<sup>[19]</sup> Thus, the use of different nucleophiles only results in a small change in the twist of the *t*Bu groups with respect to the N–S–N plane and a small shift of the halogen atom and the thf molecules for the diimidosulfonates.

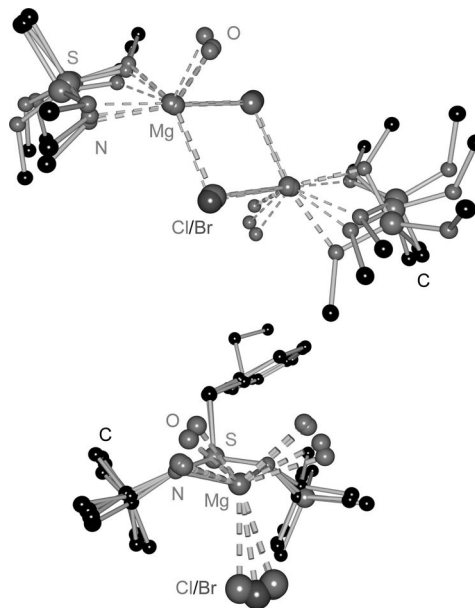


Figure 5. Top: superposition plot of **1**, **2** and **4**. All hydrogen atoms have been omitted for clarity and only the *ipso* carbon atoms of the *tert*-butyl groups and the substituents at the sulfur atoms are shown. Bottom: superposition plot of four magnesium diimidosulfonates  $[\text{MgX}(\text{N}t\text{Bu})(\text{NR}')\text{SR}]$ <sup>[19]</sup> (X = Br, R = Me, R' = *t*Bu/X = Cl, R = *n*Bu, R' = *t*Bu/X = Cl, R = Bz, R' = *t*Bu/X = Cl, R = Bz, R' = SiMe<sub>3</sub>). All hydrogen atoms and the carbon atoms of the thf have been omitted for clarity.

Figure 5 shows that the main differences between the solid-state structures of **1**, **2** and **4** involve the different arrangements of their N–S–N planes. The carbon atoms of the *t*Bu groups remain in the N–S–N plane and the configuration of the imido groups as well as the organic substituent also change very little. Both ligands are therefore skewed with respect to each other, which results in a different twist between both N–S–N planes and the central Mg<sub>2</sub>X<sub>2</sub> plane for each organic substituent.

The N–S–N planes in the structures of **1** and **2** are coplanar because of an inversion centre in the middle of the four-membered Mg<sub>2</sub>X<sub>2</sub> ring. Complexes **1** and **2** share even more similarities since they exhibit nearly the same torsion angle (74.57° vs. 75.03°) between the N–S–N planes, although there are still some differences between these two structures. For example, the deviation of the N–S–N planes out of the Mg<sub>2</sub>X<sub>2</sub> plane in **1** are larger than in **2** (50.70° vs. 35.3°) and although the torsion angles between the N–S–N planes are nearly the same in both structures, the skewing between the N–S–N planes and the Mg<sub>2</sub>X<sub>2</sub> plane is again larger in **1**.

( $90^\circ - 73.5^\circ = 16.5^\circ$ ) than in **2** ( $90^\circ - 82.3^\circ = 7.7^\circ$ ). Furthermore, it is obvious that the skewing between the two N–S–N planes and between the N–S–N planes and the  $\text{Mg}_2\text{X}_2$  plane, respectively, is greatest for **3** due to its unique structural motif (see Figure 6). Thus, the N–S–N planes in the structures of **1**, **2** and **4** are located on different sides of the central four-membered  $\text{Mg}_2\text{X}_2$  ring, with one being bent upwards and the other bent downwards, and the thf molecules and the organic substituent are in a *trans* configuration. In contrast, in **3** both these planes are located on the same side of the central ring in a *cisoid* orientation. The N–S–N planes are also heavily skewed (see Table 2) to minimise steric hindrance between the *t*Bu groups and the thf molecules and the  $\text{Mg}_2\text{X}_2$  plane is slightly folded ( $12^\circ$ ) to give the thf molecules even more room. Thus, whereas complexes **1**, **2** and **4** pack in such a way to accommodate a thf molecule in the slot between a *t*Bu group and another thf molecule of the next complex, in **3** the phenyl groups of one complex and the thf molecules of another are intertwined, which results in  $\pi\cdots\text{H}$  interactions.

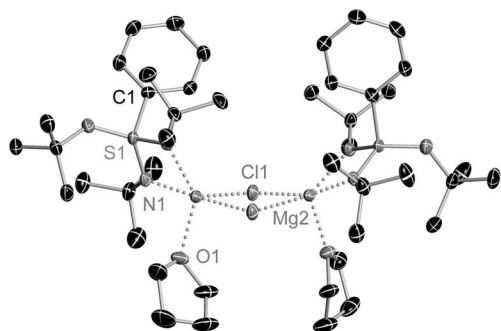


Figure 6. Crystal structure of  $[(\text{thf})\text{MgCl}(\text{N}t\text{Bu})_3\text{SPh}]_2$  (**3**). Anisotropic displacement parameters are depicted at the 50% probability level and all hydrogen atoms have been omitted for clarity.

One magnesium atom in the donor-base-free complex **5** is coordinated by two anions, thus leaving the magnesium atom with a distorted tetrahedral environment (Figure 7). The angles between the nitrogen atoms of the same anion are more acute ( $70.5^\circ$ ) than the angles between the nitrogen atoms of different anions ( $130.8^\circ$ ). The planes of the two anions coordinated to the magnesium atom are nearly perpendicular to each other ( $86.9^\circ$ ), with considerably shorter Mg–N bond lengths than those in **1–4**. This would be

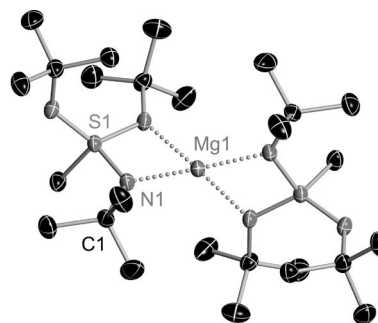


Figure 7. Crystal structure of  $[\text{Mg}\{(\text{N}t\text{Bu})_3\text{SMe}\}_2]$  (**5**). Anisotropic displacement parameters are depicted at the 50% probability level and all hydrogen atoms have been omitted for clarity.

expected since the magnesium atom is only coordinated by the two anions and no additional donor base is present. The distances in the ligand anion are the same as in **1–4**.

A similar structural motif was found by Pauer et al. in  $[(\text{thf})\text{Mg}(\text{NSiMe}_3)_2\text{SPh}]$ ,<sup>[22]</sup> where the magnesium atom is also coordinated by two anions but the use of thf as solvent and the lower steric demand of the diimidosulfonates compared to triimidosulfonates results in additional thf coordination. The magnesium atom in  $[(\text{thf})\text{Mg}\{(\text{NSiMe}_3)_2\text{SPh}\}_2]$  exhibits a square-pyramidal environment with the thf molecule occupying the apex of the pyramid. Because of the coordination geometry, the diimidosulfonate anions get very close to each other, thus resulting in considerably longer Mg–N bonds (average:  $2.14 \text{ \AA}$ ).

### NMR Investigations of the Magnesium Triimidosulfonates 1–5

Like their diimido analogues, the triimidosulfonate complexes exhibit a multiple set of the expected resonances in the NMR spectra. NMR experiments at different temperatures (see Figure 8) showed that, in contrast to the diimidosulfonates, the equilibrium between the two species in solution is not temperature-dependent. Thus, whereas the ratio between both compounds changed from 2.5:1 to 1.5:1 for the diimidosulfonates, the triimidosulfonates only exhibit negligible changes in that respect. Further NMR experiments showed that the same holds true for the time-dependence (time from preparing the sample to recording its spectrum).

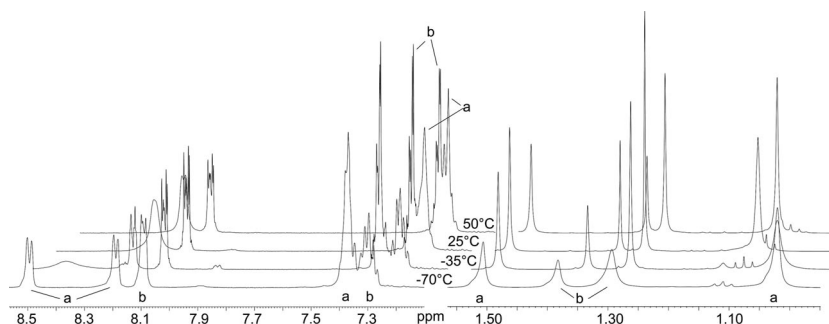


Figure 8.  $^1\text{H}$  NMR spectra of **3** at different temperatures. Left: aromatic region; right: *t*Bu signals.



Figure 8 shows that the protons of the coordinated and non-coordinated *Nt*Bu groups resonate between  $\delta = 1.0$  and 1.6 ppm, whereas the signals for the phenyl group appear between  $\delta = 7.2$  and 8.6 ppm. It is clear that the *ortho* protons of the phenyl substituent in the major component (**a**) can only be resolved at low temperature, whereas the protons of the minor component can be resolved at higher temperatures. This indicates that rotation about the S–C axis is somehow hindered in the minor component. Furthermore, the shift of the signals is noteworthy. Thus, whereas the change of the shifts for the *t*Bu protons and the organic periphery is always in the same direction (to higher or lower field) for the diimidosulfonates, the change of shifts for the triimidosulfonate signals is not uniform: as can be seen from Figure 8, the resonances for the *ortho* protons of the phenyl ring and for the protons of the non-coordinated *t*Bu group are shifted to lower field for species **b** whereas the proton signal for the coordinating *t*Bu group is shifted to higher field. The signals for the *meta/para* protons are shifted to higher field at temperatures below 0 °C and to lower field at higher temperatures. Similar shifts can be seen for compounds **2** and **4**, thus indicating that the differences between the two triimidosulfonate species in solution are greater than for the diimidosulfonate species.

A  $^{15}\text{N}$ -HMBC spectrum finally provided the solution to this puzzling observation as a cross-peak between a very broad signal that is barely visible in the  $^1\text{H}$  NMR spectrum and a  $^{15}\text{N}$ -signal which is also coupled with a *t*Bu group suggests that the protonated ligand is one of the species in solution. The hydrogen atom bonded to the nitrogen atom appears as a very broad signal at  $\delta = 3.67$  ppm, next to the thf signal. The sulfonic acid  $(t\text{BuN})_2\text{SN}(\text{H})t\text{Bu}$  is labelled as species **b** in Figure 8. As expected, the ratio of the signals for the *t*Bu groups is 2:1 for the sulfonic acid since only one nitrogen atom is protonated. A NOESY spectrum showed that exchange between the protonated nitrogen atom and the unprotonated nitrogen atoms is slow (1% of the molecules in 0.5 s). Furthermore, the identification of the sulfonic acid validates the aforementioned assumption that the difference between the two species in solution is larger for triimidosulfonates than for diimidosulfonates. Thus, whereas the latter exhibit a conformational isomerism in solution, the signal doubling for the former is due to another molecule being present in the NMR sample. In addition, this provides an explanation as to why the *ortho* protons of the phenyl substituent in **3** can be resolved for component **b** at room temperature. Since the sulfonic acid does not coordinate a metal, the angle between the two nitrogen atoms is not around 75°, as normally found for the sulfurimido metal complexes, but is much wider, which results in a hindered rotation about the S–C bond. Signals for the triimidosulfonic acid can be found in all NMR spectra of **1–5**, thus indicating that the magnesium triimidosulfonates are extremely sensitive to moisture. Even if the NMR tube is filled in the glovebox and then sealed, the spectrum still shows traces of the sulfonic acid.

Complex **1** shows an even more complex spectrum, with three components coexisting in solution. Besides the pro-

tonated  $(t\text{BuN})_2\text{SN}(\text{H})t\text{Bu}$  ligand and the signals for the magnesium triimidosulfonate, another compound, which exhibits the highest integrals, can be seen in the NMR spectrum. This major compound shows three signals, with equal integrals, for the *Nt*Bu groups rather than two signals with a 2:1 ratio (coordinating/non-coordinating), thus indicating that the molecule is arranged in such a way that it contains three non-equivalent *Nt*Bu groups. After the synthesis of  $[\text{Mg}\{(t\text{BuN})_3\text{SMe}\}_2]$ , a comparison with the NMR spectrum of **5** showed that the major compound in the spectrum of **1** is the same as in **5**, thus indicating that **1** loses magnesium bromide in solution and consequently exhibits the same structure as **5**. This also provides the reason for the three *Nt*Bu signals. As expected, one signal is due to the non-coordinated *Nt*Bu group and the crystal structure of **5** provides the reason for the difference between the coordinated groups, namely that one of them resides on the same side as the methyl group and the other opposite to another *Nt*Bu group. A DOSY spectrum of **1** confirmed that the unknown magnesium triimidosulfonate species is smaller in solution than **5**. As expected, the DOSY spectrum<sup>[23]</sup> also showed that the protonated ligand exhibits a much lower atom number and therefore moves faster in solution. A second DOSY spectrum of **2** confirmed that the triimidosulfonate species is bigger than the protonated ligand but smaller than **5**, therefore we conclude that these magnesium triimidosulfonates are monomeric in solution.

## Conclusions

We have shown that *tert*-butylsulfur triimide reacts readily with different Grignard reagents to form very pure magnesium triimidosulfonates in good yields. Complexes **1–5** should be good precursors for a variety of heterobimetallic complexes since transmetallation reactions are well established for this class of compound and the third imido group is in an ideal position to coordinate a second metal. The resulting complexes could be interesting catalysts since the tuneable organic periphery should make the complexes soluble even in non-polar solvents. Our studies have shown that the coordination geometry can easily be adapted by changing the substituent on the sulfur atom. The triimidosulfonate ligands adapt to the requirements of the added organic group by either changing the twist between both ligands in the dimer or even changing the structural motif, as shown by complexes **3** and **5**. Besides the structure in the solid state, we have also determined the likeliest conformation in solution by NMR spectroscopy. Further investigations on the coordination of a second metal by the pendant imido group are currently underway.

## Experimental Section

**General Procedures:** All experiments were carried out either in an atmosphere of purified, dry nitrogen or argon by using modified Schlenk techniques or in an argon-filled drybox. The glassware was dried for several hours at 120 °C, assembled hot and then allowed

to cool under vacuum. All solvents were freshly distilled from potassium prior to use and degassed. All reagents were available commercially or were synthesized according to published procedures [S(NtBu)<sub>2</sub>]<sup>16</sup>].

NMR spectra were recorded on a Bruker Avance 500 spectrometer. Chemical shifts are given in ppm, with positive values for low-field shifts, relative to tetramethylsilane as external standard.

Elemental analyses were performed by the Mikroanalytisches Labor des Instituts für Anorganische Chemie der Universität Göttingen with an elementar Vario EL3 apparatus. Some values deviate more than usual from the calculated ones as the substances are highly sensitive to oxygen and moisture

Mass spectra were recorded using the electron ionization method (EI-MS: 70 eV) on a Finnigan MAT 95 spectrometer. The mass-to-charge ratios (*m/z*) of the fragment ions are based on the molecular masses of the isotopes with the highest natural abundance. The molecular peak is defined as the compound with no coordinated solvent. Some spectra were unspecific as the ionic nature and lability of the synthesized compounds made measurement difficult. No electron spray ionization (ESI-MS) or fast atom bombardment (FAB-MS) mass spectra could be recorded due to the reactivity and solubility of the compounds

**Synthesis of 1–4:** S(NtBu)<sub>3</sub> (5.0 mmol) was dissolved in 20 mL of thf and 5.0 mmol of RMgX in thf (X = Cl or Br; R = Ph, Me, *n*Bu or Benzyl) was added at –78 °C over a period of 15 min. The mixture was then allowed to warm to room temperature and stirred overnight. The solvent was removed in vacuo, the residual solids re-dissolved in an *n*-hexane/THF mixture and any insoluble precipitate filtered off. The resulting solutions were stored at –24 °C to yield colourless crystals suitable for X-ray structure analyses after 1–3 days.

**5:** Complex **1** (3.0 mmol) was dissolved in 10 mL of toluene, the resulting mixture stirred for one hour and any insoluble precipitate filtered off. The resulting solution was stored at 4 °C to yield colourless crystals suitable for X-ray structure analyses after 1–3 days.

**1:** Yield 1.57 g (72%). <sup>1</sup>H NMR (500.132 MHz, [D<sub>8</sub>]THF): major compound: δ = 1.38 [s, 9 H, C(CH<sub>3</sub>)<sub>3</sub>], 1.41 [s, 9 H, C(CH<sub>3</sub>)<sub>3</sub>], 1.43 [s, 9 H, C(CH<sub>3</sub>)<sub>3</sub>], 1.77 (m, 4 H, OCH<sub>2</sub>CH<sub>2</sub>), 3.14 (s, 3 H, SCH<sub>3</sub>), 3.62 (m, 4 H, OCH<sub>2</sub>CH<sub>2</sub>) ppm. <sup>13</sup>C NMR (125.772 MHz, [D<sub>8</sub>]THF): δ = 25.3 (OCH<sub>2</sub>CH<sub>2</sub>), 33.6 [C(CH<sub>3</sub>)<sub>3</sub>], 34.0 [C(CH<sub>3</sub>)<sub>3</sub>], 34.3 [C(CH<sub>3</sub>)<sub>3</sub>], 52.5 [C(CH<sub>3</sub>)<sub>3</sub>], 53.2 (SCH<sub>3</sub>), 54.0 [C(CH<sub>3</sub>)<sub>3</sub>], 67.4 (OCH<sub>2</sub>CH<sub>2</sub>) ppm. Minor compound 1: <sup>1</sup>H NMR (500.132 MHz, [D<sub>8</sub>]THF): δ = 1.39 [br., 27 H, C(CH<sub>3</sub>)<sub>3</sub>], 3.11 (s, 3 H, SCH<sub>3</sub>) ppm. <sup>13</sup>C NMR (125.772 MHz, [D<sub>8</sub>]THF): δ = 33.7 [C(CH<sub>3</sub>)<sub>3</sub>], 52.7 [C(CH<sub>3</sub>)<sub>3</sub>], 52.8 (SCH<sub>3</sub>) ppm. Minor compound 2: <sup>1</sup>H NMR (500.132 MHz, [D<sub>8</sub>]THF): δ = 1.30 [s, 18 H, C(CH<sub>3</sub>)<sub>3</sub>], 1.34 [s, 9 H, C(CH<sub>3</sub>)<sub>3</sub>], 2.96 (s, 3 H, SCH<sub>3</sub>) ppm. <sup>13</sup>C NMR (125.772 MHz, [D<sub>8</sub>]THF): δ = 30.8 [C(CH<sub>3</sub>)<sub>3</sub>], 33.5 [C(CH<sub>3</sub>)<sub>3</sub>], 53.3 (SCH<sub>3</sub>), 53.5 [C(CH<sub>3</sub>)<sub>3</sub>] ppm. C<sub>34</sub>H<sub>76</sub>Br<sub>2</sub>Mg<sub>2</sub>N<sub>6</sub>O<sub>2</sub>S<sub>2</sub> (873.57): calcd. C 46.70, H 8.69, N 9.61, S 7.32; found C 46.34, H 8.87, N 7.91, S 5.98.

**2:** Yield 1.73 g (80%). Major compound: <sup>1</sup>H NMR (500.132 MHz, [D<sub>8</sub>]THF): δ = 0.96 (m, 3 H, CH<sub>2</sub>CH<sub>2</sub>CH<sub>2</sub>CH<sub>3</sub>), 1.37 (m, 2 H, CH<sub>2</sub>CH<sub>2</sub>CH<sub>2</sub>CH<sub>3</sub>), 1.40 [br., 27 H, C(CH<sub>3</sub>)<sub>3</sub>], 1.67 (m, 2 H, CH<sub>2</sub>CH<sub>2</sub>CH<sub>2</sub>CH<sub>3</sub>), 1.77 (m, 4 H, OCH<sub>2</sub>CH<sub>2</sub>), 3.27 (m, 2 H, CH<sub>2</sub>CH<sub>2</sub>CH<sub>2</sub>CH<sub>3</sub>), 3.62 (m, 4 H, OCH<sub>2</sub>CH<sub>2</sub>) ppm. <sup>13</sup>C NMR (125.772 MHz, [D<sub>8</sub>]THF): δ = 14.5 (CH<sub>2</sub>CH<sub>2</sub>CH<sub>2</sub>CH<sub>3</sub>), 22.4 (CH<sub>2</sub>CH<sub>2</sub>CH<sub>2</sub>CH<sub>3</sub>), 25.3 (OCH<sub>2</sub>CH<sub>2</sub>), 27.3 (CH<sub>2</sub>CH<sub>2</sub>CH<sub>2</sub>CH<sub>3</sub>), 33.3 [free C(CH<sub>3</sub>)<sub>3</sub>], 33.5 [bonded C(CH<sub>3</sub>)<sub>3</sub>], 52.5 [bonded C(CH<sub>3</sub>)<sub>3</sub>], 53.5 [free C(CH<sub>3</sub>)<sub>3</sub>], 61.5 (CH<sub>2</sub>CH<sub>2</sub>CH<sub>2</sub>CH<sub>3</sub>), 67.4 (OCH<sub>2</sub>CH<sub>2</sub>) ppm. Minor compound: δ = 0.96 (m, 3 H,

CH<sub>2</sub>CH<sub>2</sub>CH<sub>2</sub>CH<sub>3</sub>), 1.29 [s, 18 H, C(CH<sub>3</sub>)<sub>3</sub>], 1.34 [s, 9 H, C(CH<sub>3</sub>)<sub>3</sub>], (m, 2 H, CH<sub>2</sub>CH<sub>2</sub>CH<sub>2</sub>CH<sub>3</sub>), 1.82 (m, 2 H, CH<sub>2</sub>CH<sub>2</sub>CH<sub>2</sub>CH<sub>3</sub>), 2.84 (m, 2 H, CH<sub>2</sub>CH<sub>2</sub>CH<sub>2</sub>CH<sub>3</sub>) ppm. <sup>13</sup>C NMR (125.772 MHz, [D<sub>8</sub>]THF): δ = 14.3 (CH<sub>2</sub>CH<sub>2</sub>CH<sub>2</sub>CH<sub>3</sub>), 22.7 (CH<sub>2</sub>CH<sub>2</sub>CH<sub>2</sub>CH<sub>3</sub>), 30.3 (CH<sub>2</sub>CH<sub>2</sub>CH<sub>2</sub>CH<sub>3</sub>), 30.8 [protonated C(CH<sub>3</sub>)<sub>3</sub>], 33.7 [C(CH<sub>3</sub>)<sub>3</sub>], 53.1 [C(CH<sub>3</sub>)<sub>3</sub>], 54.7 [protonated C(CH<sub>3</sub>)<sub>3</sub>], 63.3 (CH<sub>2</sub>CH<sub>2</sub>CH<sub>2</sub>CH<sub>3</sub>) ppm. C<sub>40</sub>H<sub>88</sub>Cl<sub>2</sub>Mg<sub>2</sub>N<sub>6</sub>O<sub>2</sub>S<sub>2</sub> (868.80): calcd. C 55.30, H 10.21, N 9.67, S 7.38; found C 55.09, H 10.41, N 9.85, S 7.53.

**3:** Yield 1.61 g (71%). Major compound: <sup>1</sup>H NMR (500.132 MHz, [D<sub>8</sub>]THF): δ = 1.11 [s, 18 H, C(CH<sub>3</sub>)<sub>3</sub>], 1.53 [s, 9 H, C(CH<sub>3</sub>)<sub>3</sub>], 1.77 (m, 4 H, OCH<sub>2</sub>CH<sub>2</sub>), 3.62 (m, 4 H, OCH<sub>2</sub>CH<sub>2</sub>), 7.26 (br., 3 H, H<sub>metalpara</sub>/C<sub>6</sub>H<sub>5</sub>), 8.25 (d, 2 H, H<sub>ortho</sub>/C<sub>6</sub>H<sub>5</sub>) ppm. <sup>13</sup>C NMR (125.757 MHz, [D<sub>8</sub>]THF): δ = 25.3 (OCH<sub>2</sub>CH<sub>2</sub>), 32.9 [bonded C(CH<sub>3</sub>)<sub>3</sub>], 33.7 [free C(CH<sub>3</sub>)<sub>3</sub>], 52.8 [bonded C(CH<sub>3</sub>)<sub>3</sub>], 53.5 [free C(CH<sub>3</sub>)<sub>3</sub>], 67.4 (OCH<sub>2</sub>CH<sub>2</sub>), 128.0 (C<sub>para</sub>/C<sub>6</sub>H<sub>5</sub>), 129.3 (C<sub>ortho</sub>/C<sub>6</sub>H<sub>5</sub>), 129.3 (C<sub>meta</sub>/C<sub>6</sub>H<sub>5</sub>), 153.3 (C<sub>ipso</sub>/C<sub>6</sub>H<sub>5</sub>) ppm. Minor compound: <sup>1</sup>H NMR (500.132 MHz, [D<sub>8</sub>]THF): δ = 1.31 [s, 18 H, C(CH<sub>3</sub>)<sub>3</sub>], 1.35 [s, 9 H, C(CH<sub>3</sub>)<sub>3</sub>], 7.32 (m, 3 H, H<sub>metalpara</sub>/C<sub>6</sub>H<sub>5</sub>), 8.10 (m, 2 H, H<sub>ortho</sub>/C<sub>6</sub>H<sub>5</sub>) ppm. <sup>13</sup>C NMR (125.757 MHz, [D<sub>8</sub>]THF): δ = 31.4 [protonated C(CH<sub>3</sub>)<sub>3</sub>], 33.3 [C(CH<sub>3</sub>)<sub>3</sub>], 53.6 [C(CH<sub>3</sub>)<sub>3</sub>], 55.4 [protonated C(CH<sub>3</sub>)<sub>3</sub>], 128.2 (C<sub>para</sub>/C<sub>6</sub>H<sub>5</sub>), 129.0 (C<sub>ortho</sub>/C<sub>6</sub>H<sub>5</sub>), 129.9 (C<sub>meta</sub>/C<sub>6</sub>H<sub>5</sub>), 153.3 (C<sub>ipso</sub>/C<sub>6</sub>H<sub>5</sub>) ppm. C<sub>44</sub>H<sub>80</sub>Cl<sub>2</sub>Mg<sub>2</sub>N<sub>6</sub>O<sub>2</sub>S<sub>2</sub> (908.78): calcd. C 58.20, H 8.90, N 9.30, S 7.10; found C 57.00, H 8.50, N 9.00, S 6.80.

**4:** Yield 1.82 g (78%). <sup>1</sup>H NMR (500.134 MHz, [D<sub>8</sub>]THF): major compound: δ = 1.38 [s, 18 H, C(CH<sub>3</sub>)<sub>3</sub>], 1.44 [s, 9 H, C(CH<sub>3</sub>)<sub>3</sub>], 1.77 (m, 4 H, OCH<sub>2</sub>CH<sub>2</sub>), 3.62 (m, 4 H, OCH<sub>2</sub>CH<sub>2</sub>), 4.59 (s, 2 H, CH<sub>2</sub>Ph), 7.27 (m, 3 H, H<sub>metalpara</sub>/C<sub>6</sub>H<sub>5</sub>), 7.66 (d, 2 H, H<sub>ortho</sub>/C<sub>6</sub>H<sub>5</sub>) ppm. <sup>13</sup>C NMR (125.757 MHz, [D<sub>8</sub>]THF): δ = 25.3 (OCH<sub>2</sub>CH<sub>2</sub>), 33.4 [bonded C(CH<sub>3</sub>)<sub>3</sub>], 33.5 [free C(CH<sub>3</sub>)<sub>3</sub>], 52.8 [C(CH<sub>3</sub>)<sub>3</sub>], 67.4 (OCH<sub>2</sub>CH<sub>2</sub>), 68.4 (CH<sub>2</sub>Ph), 127.7 (C<sub>para</sub>/C<sub>6</sub>H<sub>5</sub>), 128.4 (C<sub>ortho</sub>/C<sub>6</sub>H<sub>5</sub>), 132.0 (C<sub>meta</sub>/C<sub>6</sub>H<sub>5</sub>), 136.1 (C<sub>ipso</sub>/C<sub>6</sub>H<sub>5</sub>) ppm. Minor compound: <sup>1</sup>H NMR (500.132 MHz, [D<sub>8</sub>]THF): δ = 1.32 [s, 18 H, C(CH<sub>3</sub>)<sub>3</sub>], 1.34 [s, 9 H, C(CH<sub>3</sub>)<sub>3</sub>], 4.10 (s, 2 H, CH<sub>2</sub>Ph), 7.06 (m, 3 H, H<sub>metalpara</sub>/C<sub>6</sub>H<sub>5</sub>), 7.53 (d, 2 H, H<sub>ortho</sub>/C<sub>6</sub>H<sub>5</sub>) ppm. <sup>13</sup>C NMR (125.757 MHz, [D<sub>8</sub>]THF): δ = 33.4 [C(CH<sub>3</sub>)<sub>3</sub>], 33.6 [protonated C(CH<sub>3</sub>)<sub>3</sub>], 54.1 [C(CH<sub>3</sub>)<sub>3</sub>], 69.5 (CH<sub>2</sub>Ph), 127.9 (C<sub>para</sub>/C<sub>6</sub>H<sub>5</sub>), 128.3 (C<sub>ortho</sub>/C<sub>6</sub>H<sub>5</sub>), 132.0 (C<sub>meta</sub>/C<sub>6</sub>H<sub>5</sub>), 136.1 (C<sub>ipso</sub>/C<sub>6</sub>H<sub>5</sub>) ppm. C<sub>46</sub>H<sub>84</sub>Cl<sub>2</sub>Mg<sub>2</sub>N<sub>6</sub>O<sub>2</sub>S<sub>2</sub> (936.83): calcd. C 58.90, H 8.90, N 8.90, S 6.80; found C 58.50, H 9.10, N 9.20, S 6.70.

**5:** Yield 1.27 g (90%). Major compound: <sup>1</sup>H NMR (500.132 MHz, [D<sub>8</sub>]THF): δ = 1.38 [s, 9 H, C(CH<sub>3</sub>)<sub>3</sub>], 1.41 [s, 9 H, C(CH<sub>3</sub>)<sub>3</sub>], 1.43 [s, 9 H, C(CH<sub>3</sub>)<sub>3</sub>], 3.14 (s, 3 H, SCH<sub>3</sub>) ppm. <sup>13</sup>C NMR (125.772 MHz, [D<sub>8</sub>]THF): δ = 33.6 [C(CH<sub>3</sub>)<sub>3</sub>], 34.0 [C(CH<sub>3</sub>)<sub>3</sub>], 34.3 [C(CH<sub>3</sub>)<sub>3</sub>], 52.5 [C(CH<sub>3</sub>)<sub>3</sub>], 53.2 (SCH<sub>3</sub>), 54.0 [C(CH<sub>3</sub>)<sub>3</sub>] ppm. <sup>15</sup>N NMR (40.548 MHz, [D<sub>8</sub>]THF): δ = –258.1 [NC(CH<sub>3</sub>)<sub>3</sub>], –259.1 [NC(CH<sub>3</sub>)<sub>3</sub>] ppm. Minor compound: <sup>1</sup>H NMR (500.132 MHz, [D<sub>8</sub>]THF): δ = 1.30 [s, 18 H, C(CH<sub>3</sub>)<sub>3</sub>], 1.34 [s, 9 H, C(CH<sub>3</sub>)<sub>3</sub>], 2.96 (s, 3 H, SCH<sub>3</sub>) ppm. <sup>13</sup>C NMR (125.772 MHz, [D<sub>8</sub>]THF): δ = 30.8 [protonated C(CH<sub>3</sub>)<sub>3</sub>], 33.5 [C(CH<sub>3</sub>)<sub>3</sub>], 53.3 (SCH<sub>3</sub>), 53.5 [C(CH<sub>3</sub>)<sub>3</sub>] ppm. <sup>15</sup>N NMR (40.548 MHz, [D<sub>8</sub>]THF): δ = –253.1 [NHC(CH<sub>3</sub>)<sub>3</sub>], –261.2 [NC(CH<sub>3</sub>)<sub>3</sub>] ppm. C<sub>26</sub>H<sub>60</sub>MgN<sub>6</sub>S<sub>2</sub> (545.23): calcd. C 57.27, H 11.09, N 15.41, S 11.76; found C 54.71, H 10.56, N 14.66, S 10.73.

**X-ray Crystal Structure Determinations:** Data for **1–5** were collected for shock-cooled crystals at 100 K (133 K for **4**).<sup>[24]</sup> Data for **1–3** and **5** were collected with a Bruker SMART-APEX II diffractometer fitted with a D8 goniometer. A rotating anode was used as the X-ray source for data collection with **1** and **2** and an Incoatec microfocus source was utilized for **3** and **5**.<sup>[25]</sup> Data for complex **4** were collected using a Stoe IPDS II diffractometer with

Table 3. Crystallographic data for compounds 1–4.

Compound	1	2	3	4	5
Formula	C <sub>34</sub> H <sub>76</sub> Br <sub>2</sub> Mg <sub>2</sub> O <sub>2</sub> N <sub>6</sub> S <sub>2</sub>	C <sub>40</sub> H <sub>88</sub> Cl <sub>2</sub> Mg <sub>2</sub> O <sub>2</sub> N <sub>6</sub> S <sub>2</sub>	C <sub>44</sub> H <sub>80</sub> Cl <sub>2</sub> Mg <sub>2</sub> O <sub>2</sub> N <sub>6</sub> S <sub>2</sub>	C <sub>46</sub> H <sub>84</sub> Cl <sub>2</sub> Mg <sub>2</sub> O <sub>2</sub> N <sub>6</sub> S <sub>2</sub>	C <sub>26</sub> H <sub>60</sub> MgN <sub>6</sub> S <sub>2</sub>
<i>M</i>	873.57	868.80	908.78	936.83	545.23
<i>T</i> [K]	100	170	100	133	100
Space group	<i>Pbca</i>	<i>P1̄</i>	<i>P2<sub>1</sub>2<sub>1</sub>2<sub>1</sub></i>	<i>P1̄</i>	<i>C2/c</i>
<i>a</i> [Å]	13.422(3)	9.228(1)	11.126(1)	12.322(3)	26.111(5)
<i>b</i> [Å]	14.870(3)	9.340(1)	16.388(2)	14.472(3)	8.623(2)
<i>c</i> [Å]	22.040(5)	15.356(2)	27.660(2)	15.409(3)	17.960(3)
<i>α</i> [°]	90	80.931(2)	90	75.81(3)	90
<i>β</i> [°]	90	76.870(2)	90	88.29(3)	125.825(11)
<i>γ</i> [°]	90	73.427(2)	90	77.26(3)	90
<i>V</i> [Å <sup>3</sup> ]	4398.8(17)	1229.3(2)	5043.9(7)	2597.6(9)	3278.6(11)
<i>Z</i>	4	1	4	2	4
<i>θ</i> range [°]	2.24–25.35	2.29–25.39	2.21–25.31	1.69–26.02	1.92–25.17
Data	33816	9031	35965	26612	27048
Unique data	4044	4528	9233	10222	5773
<i>R</i> <sub>int</sub>	0.0270	0.0392	0.0528	0.1014	0.0994
<i>R</i> <sub>1</sub>	0.0376	0.0634	0.0472	0.0713	0.1011
<i>wR</i> <sub>2</sub>	0.0743	0.1301	0.0792	0.1404	0.1842
Parameters	258	254	633	569	170
GooF	1.055	1.072	1.026	0.998	1.029
Peak/hole [e/Å <sup>3</sup> ]	0.661/–0.858	0.544/–0.497	0.272/–0.271	0.617/–0.663	0.400/–0.710

a sealed tube and an image plate detector. All diffractometers were equipped with a low-temperature device and used monochromated Mo-*K*<sub>α</sub> radiation ( $\lambda = 0.71073$  Å). The Incoatec microfocus source and the rotating anode used mirror optics as radiation monochromator whereas the sealed tube devices used a graphite monochromator. Data for 1–3 and 5 were integrated with SAINT,<sup>[26]</sup> and an empirical absorption correction (SADABS)<sup>[27]</sup> was applied. Data collection and data reduction for 4 were performed with X-Area.<sup>[28]</sup> All structures were solved by direct methods (SHELXS-97)<sup>[29]</sup> and refined by full-matrix least-squares methods against *F*<sup>2</sup> (SHELXL-97).<sup>[30]</sup> All non-hydrogen atoms were refined with anisotropic displacement parameters. The hydrogen atoms were refined isotropically at calculated positions using a riding model with their *U*<sub>iso</sub> values constrained to 1.5 times the *U*<sub>eq</sub> of their pivot atoms for terminal sp<sup>3</sup> carbon atoms and 1.2 times for all other carbon atoms. Disordered moieties were refined using bond-length restraints and isotropic displacement parameter restraints.<sup>[31]</sup> The Flack parameter<sup>[32]</sup> for 3 could not be determined successfully because of racemic twinning. Further details can be found in Table 3.

CCDC-761798 (for 1), -761799 (for 2), -761800 (for 3), -761801 (for 4) and -761802 (for 5) contain the supplementary crystallographic data for this paper. These data can be obtained free of charge from The Cambridge Crystallographic Data Centre via [www.ccdc.cam.ac.uk/data\\_request/cif](http://www.ccdc.cam.ac.uk/data_request/cif).

## Acknowledgments

This work was supported by the Deutsche Forschungsgemeinschaft (DFG) within the priority program 1178 (“Experimental charge density as the key to understanding chemical interactions”) and Chemetall GmbH (Frankfurt and Langelsheim).

- [1] F. A. Cotton, G. Wilkinson, C. A. Murillo, M. Bochmann, *Advanced Inorganic Chemistry*, John Wiley & Sons, Inc., New York, 1999.  
 [2] M. Goehring, G. Weis, *Angew. Chem.* **1956**, 68, 678.

- [3] O. Glemser, J. Wegener, *Angew. Chem.* **1970**, 82, 324; *Angew. Chem. Int. Ed. Engl.* **1970**, 9, 309.  
 [4] S. Pohl, B. Krebs, U. Seyer, G. Henkel, *Chem. Ber.* **1979**, 112, 1751–1755.  
 [5] a) R. Fleischer, S. Freitag, F. Pauer, D. Stalke, *Angew. Chem.* **1996**, 108, 208–211; *Angew. Chem. Int. Ed. Engl.* **1996**, 35, 204–208; b) R. Fleischer, A. Rothenberger, D. Stalke, *Angew. Chem.* **1997**, 109, 1141–1143; *Angew. Chem. Int. Ed. Engl.* **1997**, 36, 1105–1107.  
 [6] R. Fleischer, S. Freitag, D. Stalke, *J. Chem. Soc., Dalton Trans.* **1998**, 193–197.  
 [7] O. Glemser, S. Pohl, F.-M. Tesky, R. Mews, *Angew. Chem.* **1977**, 89, 829–830; *Angew. Chem. Int. Ed. Engl.* **1977**, 16, 789–790.  
 [8] W. Lidy, W. Sundermeyer, W. Verbeek, *Z. Anorg. Allg. Chem.* **1974**, 406, 228–234.  
 [9] a) J. K. Brask, T. Chivers, M. Parvez, G. P. A. Yap, *Inorg. Chem.* **1999**, 38, 3594–3595; b) J. K. Brask, T. Chivers, M. Parvez, *Angew. Chem.* **2000**, 112, 988–990; *Angew. Chem. Int. Ed.* **2000**, 39, 958–960; c) J. K. Brask, T. Chivers, *Angew. Chem.* **2001**, 113, 4082–4098; *Angew. Chem. Int. Ed.* **2001**, 40, 3960–3976.  
 [10] a) S. L. Hinchley, P. Trickey, H. E. Robertson, B. A. Smart, D. W. H. Rankin, D. Leusser, B. Walford, D. Stalke, M. Bühl, S. J. Obrey, *J. Chem. Soc., Dalton Trans.* **2002**, 4607–4616; b) J. Henn, D. Ilge, D. Leusser, D. Stalke, B. Engels, *J. Phys. Chem. A* **2004**, 108, 9442–9452.  
 [11] D. Leusser, B. Walford, D. Stalke, *Angew. Chem.* **2002**, 114, 2183–2186; *Angew. Chem. Int. Ed.* **2002**, 41, 2079–2082.  
 [12] D. Leusser, J. Henn, N. Kocher, B. Engels, D. Stalke, *J. Am. Chem. Soc.* **2004**, 126, 1781–1793.  
 [13] a) R. Fleischer, D. Stalke, *Chem. Commun.* **1998**, 343–345; b) R. Fleischer, D. Stalke, *Organometallics* **1998**, 17, 832–838; c) R. Fleischer, D. Stalke, *J. Organomet. Chem.* **1998**, 550, 173–182.  
 [14] a) R. Fleischer, D. Stalke, *Coord. Chem. Rev.* **1998**, 176, 431–450; b) R. Fleischer, B. Walford, A. Gbureck, P. Scholz, W. Kiefer, D. Stalke, *Chem. Eur. J.* **1998**, 4, 2266–2279; c) B. Walford, D. Stalke, *Angew. Chem.* **2001**, 113, 3965–3969; *Angew. Chem. Int. Ed.* **2001**, 40, 3846–3849.  
 [15] D. Stalke, *Proc. Ind. Acad. Sci.* **2000**, 112, 155–170.  
 [16] B. Walford, A. P. Leedham, C. R. Russell, D. Stalke, *Inorg. Chem.* **2001**, 40, 5668–5674.

- [17] C. Selinka, D. Stalke, *Eur. J. Inorg. Chem.* **2003**, 3376–3382.
- [18] R. G. Pearson, *J. Am. Chem. Soc.* **1963**, 85, 3533–3539.
- [19] T. Schulz, S. Deuerlein, D. Stalke, *Eur. J. Inorg. Chem.* **2010**, 2178–2184, preceding paper.
- [20] a) S. Handa, K. Nagawa, Y. Sohtome, S. Matsunaga, M. Shibasaki, *Angew. Chem.* **2008**, 120, 3274–3277; *Angew. Chem. Int. Ed.* **2008**, 47, 3230–3233; b) S. Podder, J. Choudhury, S. Roy, *J. Org. Chem.* **2007**, 72, 3129; c) G. Bai, S. Singh, H. W. Roesky, M. Noltemeyer, H.-G. Schmidt, *J. Am. Chem. Soc.* **2005**, 127, 3449–3455.
- [21] a) C. Selinka, S. Deuerlein, T. Häuser, D. Stalke, *Inorg. Chim. Acta* **2004**, 357, 1873–1880; b) B. Walfort, T. Auth, B. Degel, H. Helten, D. Stalke, *Organometallics* **2002**, 21, 2208–2214.
- [22] S. Freitag, W. Kolodziejewski, F. Pauer, D. Stalke, *J. Chem. Soc., Dalton Trans.* **1993**, 3479–3488.
- [23] a) I. Fernández, E. Martínez-Viviente, F. Breher, P. S. Pregosin, *Chem. Eur. J.* **2005**, 11, 1495–1506; b) H. Barjat, G. A. Morris, S. Smart, A. G. Swanson, S. C. R. Williams, *J. Magn. Reson., Ser. B* **1995**, 108, 170–172.
- [24] a) D. Stalke, *Chem. Soc. Rev.* **1998**, 27, 171–178; b) T. Kottke, D. Stalke, *J. Appl. Crystallogr.* **1993**, 26, 615–619; c) T. Kottke, R. J. Lagow, D. Stalke, *J. Appl. Crystallogr.* **1996**, 29, 465–468.
- [25] T. Schulz, K. Meindl, D. Leusser, D. Stern, J. Graf, C. Michaelsen, M. Ruf, G. M. Sheldrick, D. Stalke, *J. Appl. Crystallogr.* **2009**, 42, 885–891.
- [26] Bruker, *SAINT*, v7.34A, Bruker AXS Inc., Madison, WI, USA, **2005**.
- [27] G. M. Sheldrick, *SADABS* **2008/2**, Göttingen, **2008**.
- [28] *X-AREA*, Stoe & Cie GmbH, Darmstadt, **2002**.
- [29] G. M. Sheldrick, *Acta Crystallogr., Sect. A* **1990**, 46, 467–473.
- [30] G. M. Sheldrick, *Acta Crystallogr., Sect. A* **2008**, 64, 112–122.
- [31] P. Müller, R. Herbst-Irmer, A. L. Spek, T. R. Schneider, M. R. Sawaya, in: *Crystal Structure Refinement - A Crystallographer's Guide to SHELXL*, in: *IUCr Texts on Crystallography*, vol. 8 (Eds.: P. Müller), Oxford University Press, Oxford (England), **2006**.
- [32] H. D. Flack, *Acta Crystallogr., Sect. A* **1983**, 39, 876–881.

Received: January 18, 2010  
Published Online: April 7, 2010